

Assessment of Rock Slope Weathering Based on the Alteration of Photogrammetric Roughness Data

D-H. Kim¹, I. Gratchev², E. Oh³ and A.S. Balasubramaniam⁴
^{1,2,3,4}Griffith School of Engineering, Griffith University, Gold Coast, Australia
 E-mail: donghyun.kim@griffith.edu.au

ABSTRACT: This article presents a method to identify the durability of rocks from weathering through annual photogrammetry surveys. The weathering of rock slopes can be visually investigated with exposed joint structural data, which are features obtained from the information of joint spacing and thickness, as well as with the durability and the constituents of rock types. Close range digital photogrammetry can create high resolution 3D models and also records the structural data of rock slopes as time progresses. In this study, photogrammetric surveys were conducted with two year intervals on a highly weathered rock slope for the monitoring of weathering. The joint roughness coefficients (JRC), which were obtained from slope surfaces including major joint sets, were quantified by means of the digitized profile data extracted from the photogrammetric 3D models. By comparing photogrammetric 3D images over the selected two year period, it was found that the changes of JRC values adjacent to the exposed joints on the rock surfaces patently indicated the influence of weathering within a short term comparison. In this study, JRC variation rate (JVR) is suggested to identify the durability of rock slope materials based on the correlation between the surface roughness and the durability of rock materials.

KEYWORDS: Photogrammetry, Weathering, JRC variation rate (JVR)

1. INTRODUCTION

The weathering of rock surface fractures accelerates other failures within the rock surfaces which are important features in engineering works for the long-term stability of rock slopes. The weathering grades and the weathering rates of rock material have thus been of significant interest to geologists and engineers. From a geological perspective, rock weathering is normally approached using qualitative methods. Many weathering indices have been investigated and these indices are generally derived from chemical and mineralogical analysis. From an engineering point of view, weathering is studied using quantitative approaches rather than geological approaches, where rock masses are classified based on the durability and the strength of the rock mass in respect to the degree of weathering.

In both cases, the identification of weathering is preferentially conducted by visual observations from exposed rock surfaces. The description of weathering by visual observations is frequently subjective and ambiguous. On the basis of the weathering process, the degree of weathering has been thus investigated to be quantified by measuring the degree of jointing, which is related to the number of joint sets and joint spacings. Based on this principle, the degree of jointing has been investigated to quantify weathering degrees (Ehlen, 1999; Marinos et al., 2005; Kim et al., 2014).

In these studies, the geological strength index (GSI), which is estimated from visual observation of exposed outcrops, was effectively used as a representative indicator supporting the characterization of the rock mass with consideration to weathering (Heok & Brown, 1997; Cai & Kaiser, 2006). Cai & Kaiser (2006) suggested a quantitative function, where joint roughness parameters are used for the determination of GSI values. These values are generally obtained from joint sets in both large and small scales. With consideration of the influence of weathering, the roughness parameters can be the most dominant factors since rock surfaces and their joint sets are directly exposed to a weathering environment.

As an indicator of the degree of weathering, many studies have attempted to analyze rock surface roughness combined with the weathering states (McCarroll & Nesje, 1996; White et al., 1998; Gómez-Pujol et al., 2006; Pinho et al., 2006; Medapati et al., 2013). McCarroll and Nesje (1996) suggested that roughness is a useful indicator to quantify the degree of weathering through a set of measurements of roughness profiles using profile gauges. Using the triangulate point clouds obtained from a laser scanned 3D model, Medapati et al. (2013) attempted to use the γ -values, which are the

angles from the vertical axis to the normal vector, for identifying the rock surface roughness in different weathering conditions.

In rock engineering, the rock joint roughness coefficients (JRC) are significant engineering values for describing the mechanical and the hydrological properties of rock joints. The values are generally obtained from rock slopes or boring logs using manual measurements. However, close range photogrammetry has successfully attempted to obtain JRC values for many purposes (Poropat, 2009; Kim et al., 2013, 2014). Even though the accuracy of photogrammetric 3D models for JRC estimation has not been sufficiently established, photogrammetry enables surveys of roughness data over large areas of rock slopes.

In this study, photogrammetric JRC data has been collected over a two-year period between 2012 and 2014. With the comparisons of the annual JRC data with the durability of rocks, JRC variation rates were investigated to suggest an index to quantify the weathering degree for engineering purposes. The JRC values were calculated using digitized roughness profiles extracted from photogrammetric 3D models, which included exposed joint sets.

2. APPLICATION OF PHOTOGRAMMETRY

2.1 Fundamental of photogrammetry

Photogrammetric models are created by the calculation of the 3D coordinates of both images based on the employed camera parameters and ground control points as shown in Figure 1. This can be explained as the concept of stereoscopic parallax, which is the position change of an object with respect to the changed camera locations.

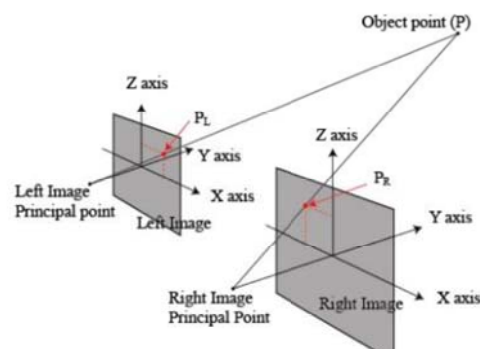


Figure 1 Geometry for the determination of the position of a point object space using photogrammetry (Poropat, 2006)

In the 3D coordinate system, the x coordinates of the point P on both images are differently indicated by P_L and P_R . Thus, the 3D position of the point P can be identified using relationships between the relative positions obtained from the images and the camera perspective centre.

2.2 Limitations of photogrammetric 3D models

Photogrammetry produces 3D models based on the collected data from a given range of view angles. Therefore, the exposed joint lines on rock surface joints are not sufficiently created in 3D models, as shown in Figure 2 (a). The depth accuracy of 3D images generally depends on base-to-distance ratio, which is the distance ratio between baseline distances and camera-to-object distances. However, it is not easy to define the depth accuracy for all targeted joint sets on a 3D model since the locations of the targeted joints are various.

Photogrammetric 3D models simulate joint planes based on the clearly extended planes or the extruded parts of the joint planes from the rock slope surfaces. Due to the limitation of the camera's view and the brightness of the joint space, the inside information between joints is rarely created and the creation is dependent on the thickness of the joints. However, when a roughness profile of an exposed joint set is changed by weathering, the loss of roughness between the joint edges can be measured from the roughness profiles as presented in Figure 2 (b).

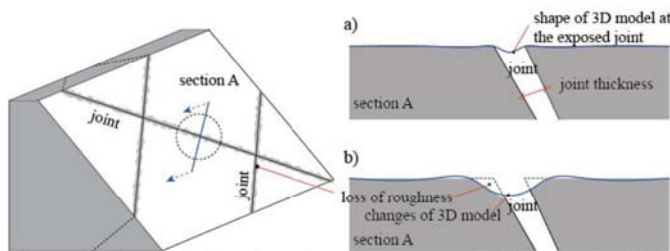


Figure 2 Schematic drawing of a photogrammetric 3D model of the intersection of a joint, before weathering (a), and after loss of roughness by weathering (b)

3. ESTIMATION ROCK SURFACE ROUGHNESS

3.1 Estimation of directional JRCs

Using the two dimensional roughness profiles, JRC values can be calculated using roughness parameters. Based on Barton's typical JRC values, the following two extrapolate functions suggested by Maerz et al. (1990) and Tse and Cruden (1979), have been widely employed to estimate JRC values using digitized profile coordinates.

$$JRC = 32.2 + 32.47 \log Z_2 \quad (\text{Tse and Cruden, 1979}) \quad (1)$$

$$JRC = 411(R_p - 1) \quad (\text{Maerz et al., 1990}) \quad (2)$$

where Z_2 is a roughness parameter using variances within asperity heights and R_p is also a roughness parameter which is related to the inclination angle (i) of the sawtooth surface of the roughness profiles. With consideration to quantifying the degree of weathering, JRC values can be employed to calculate GSI values. Cai and Kaiser (2006) proposed a quantitative method to estimate GSI values using the relationship between the joint condition factor (J_c), joint alteration number (J_A) and block volumes (V_b) in a three dimensional space as shown in Eq. (3) and Eq. (4):

$$GSI = \frac{26.5 + 8.79 \ln J_c + 0.9 \ln V_b}{1 + 0.0151 \ln J_c - 0.0253 \ln V_b} \quad (3)$$

$$J_c = \frac{J_w J_s}{J_A} \quad (4)$$

where J_s is a term to describe small scale smoothness and J_w is a factor to describe large scale waviness of joints. J_s is closely related

to JRC values (Palmström, 2001) and the linear relationship between these two parameters has been suggested by Kim et al. (2014) as presented in Eq. (5).

$$J_s = 0.1125 \times JRC + 0.75 \quad (5)$$

JRC values describe the roughness of joint sets. In this study, JRC values are employed to estimate the roughness of the profiles, including the intersection joints with rock slope surfaces, as demonstrated in Figure 2.

3.2 Influence of the alteration of roughness

If a rock type is vulnerable to weathering, the variations of roughness on the exposed rock slopes can be mostly observed at the intersections of the exposed joints within the surface areas of slopes in a short term period. Weathering typically erodes the edges of joints. Depending on the geological components of rocks, the roughness alterations will produce the different forms of weathering products. Typically, the exposed edges of joints become rounded. Therefore, it is generally accepted that loss of roughness leads to a decrease of JRC values of the areas. However, the decrease in JRC values are not necessarily proportionate to the loss of roughness. Indeed, a partial loss of roughness in a specific area along a joint may actually produce an increase of JRC values.

Similarly, in the case of laminated structure rocks such as shales and mudstones, exfoliations with a shape of flakes can be more dominant than other types of breaks. The partial exfoliations with the shapes of flakes can cause a significant increase in JRC values of rock surfaces due to the step-like profiles on the altered surfaces near joint intersections. Therefore, it can be said that the JRC variations by the weathering process can reflect the geological structural characteristics of the rock material as well as its durability. To establish the indicator, this study suggests a JRC variation rate (JVR) as presented in Eq. (6). This can be obtained by the comparison of JRC values collected from annual investigations. In order to collect sufficient data and to cover the investigations in large slope surface areas, remote sensing methods such as photogrammetry methods, can be more efficiently used for the historical JRC records.

$$JRC \text{ variation rate (JVR)} = ((JRC_{12} - JRC_{11}) / JRC_{11}) / \text{year} \quad (6)$$

where JRC_{11} is the previously measured value in a particular year and JRC_{12} is a measured value at present. Thus, if the JRC variations are negative, the roughness values have been decreased during the specific periods. In consideration of the measurement accuracies of 3D models, collected JRC variation rates can be evaluated by statistical methods. As presented by Medapati et al. (2013), roughness data can form specific distributions according to their weathering condition. Accordingly, JVR data can show different shapes of distribution curves depending on the structure and durability of rock material. The data distributions are distinguished by several statistical indices such as mean, median and skew (see Figure 3). It is worth mentioning that the statistical indices obtained from the annually observed data can supplement weathering characteristics with reasonable correlations with the durability indices of the rocks.

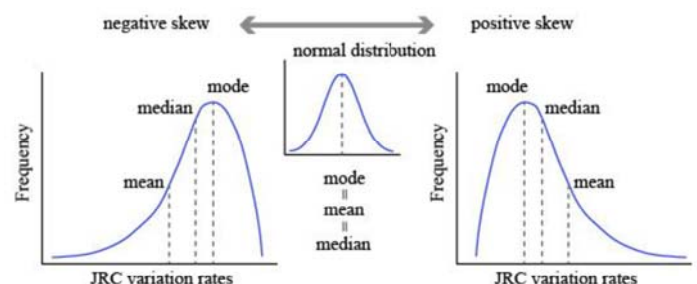


Figure 3 Examples of data distributions

4. GEOLOGICAL CONDITIONS OF THE STUDY AREA AND STRENGTH PROPERTIES OF ROCKS

The study area is located on the eastern road near Tamborine mountain in Australia which is composed of sandstone and shale in the Naranleigh-Fernvale beds (Gratchev et al., 2013). The rocks are heavily weathered and the composed bedding is steeply inclined. The geological structures are alternate layers of sandstone beds and shale. The slope height is around 8 metres and the length extends up to 200 metres. Before the beginning of the photogrammetry surveys, the slope experienced failures during heavy rainfall. Thus, the photogrammetry surveys were performed on the freshly exposed rock joint surfaces.

Using collected lump samples from the site, point load tests and slake durability tests were performed. The unconfined compressive strengths (UCS) were estimated from the results of the point load tests. As an approximated conversion factor, 24 was used to estimate the UCS values (Broch and Franklin, 1972). The average values of UCS were 70.6 MPa and 16.2 MPa for both the shale and the sandstone samples respectively. A total of 40 Schmidt hammer tests were also performed on the discontinuities of the shale and sandstone areas. Table 1 presents the results of these tests which are classified as weathering grades III and IV for both the shale and sandstone areas respectively. The weathering grades were classified based on the experimental study performed by Arikan et al., (2007). The test results are demonstrated in the author's previous research in detail (Kim et al., 2014).

Figure 4 classifies the tested rock samples based on their point load strengths (Broch and Franklin, 1972). In the present study, the slake durability values of the samples are also compared with the unconfined compressive strengths. The sandstone samples collected from the site have a low durability of around 50% of Id_2 . Because the texture of the sample surfaces is composed of coarse sand grains, the samples considerably lost weight during the slaking procedure with rounded surfaces. In the case of shale samples, on the other hand, a high range of Id_2 value (92.5 %) was obtained using weathered samples, even though they had low UCS values. The durability of shale samples is classified as 'high' to 'extremely high' durability according to the slake durability index (Franklin and Chandra, 1972). The results were as expected: relatively more loss of weight from the sandstone surfaces could be observed than the shale zone in the same period.

Table 1 Results of Schmidt hammer tests (Kim et al., 2014)

Rock types	Schmidt hammer rebounds			Weathering grades
	Range of data	Mean	SD	
Shale	17 ~ 49	31.3	8.3	III (20 ~ 30)
Sandstone	11 ~ 46	27.7	10.9	IV (30 ~ 40)

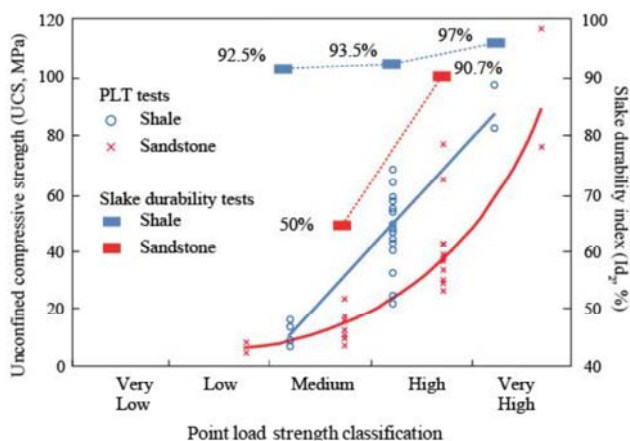


Figure 4 Unconfined compressive strength (UCS) and slake durability index (Id_2) according to point strength classification

5. PHOTOGRAMMETRY SURVEYS

5.1 Camera networks

Two photogrammetry surveys were carried out on the same slope site within a two year time period. A normal digital camera (Nikon D7000) with a fixed focal length lens (FL=24mm) was employed to capture the slope images. As shown in Figure 5, the images were captured from two camera positions. The camera locations and the camera-to-object distances were kept constant for creating 3D images under the same survey conditions. The baseline distance, 2.5 metres, was selected based on the desirable base-to-distance ratio range (1:6 to 1:10) for the employed photogrammetry software (Sirovision).

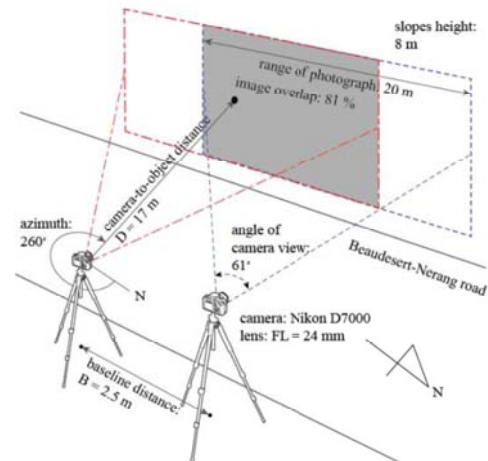


Figure 5 Camera setup

5.2 3D surface models

The photogrammetry code "Sirovision (CSIRO, 2012)" was employed to create 3D images. Geo-referencing was performed for the two different 3D models by giving the coordinates of the left camera position (using a GPS device) and measuring its bearing to the centre of the slope (using a geological compass). Figure 6 shows 2012 3D models of both selected shale and sandstone zones for JRC estimations.

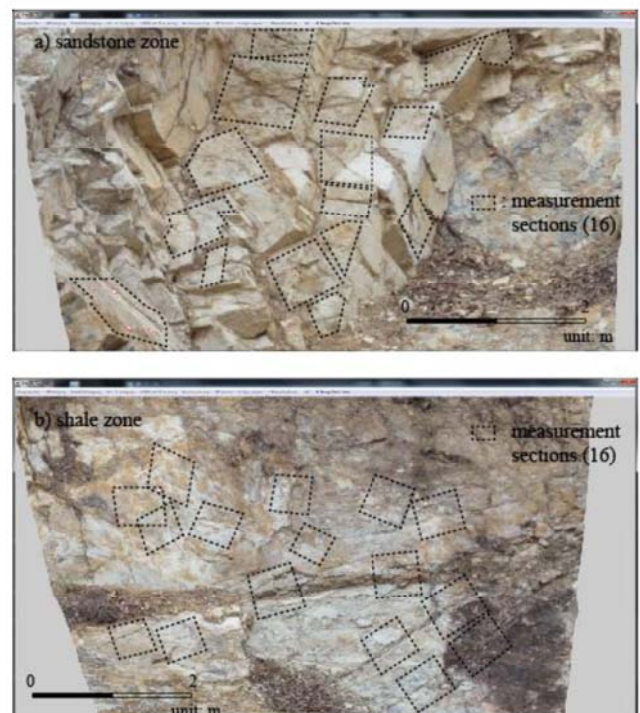


Figure 6 Photogrammetric 3D models (surveyed in 2012) and selected surface areas, sandstone (a), shale (b)

5.3 Alteration of surface roughness

With visual comparisons of the 3D models of 2012 and 2014, it was found that there had been roughness alterations, especially on the periphery of exposed joints in both rock zones. The images show a large alteration of colours on the surfaces in the shale sections. This exfoliation phenomenon was not found in the slake durability tests. An example of the changes is presented in Figure 7 (a, b). This alteration was accompanied by the exfoliation of thin rock flakes. In sandstone sections, however, dominant changes occurred around the edges of joints as shown in Figure 7 (c, d). It was also found that in both rock types, several sections lost large portions of surface roughness resulting in large variations of profile shapes.



Figure 7 Examples of the 3D image cuts showing the alteration of rock surfaces due to weathering process over two years; shale, section 2 (a, b), sandstone, section 4 (c, d)

JRC values were estimated in 16 measurement sections in both rock types respectively. As shown in Figure 8, the measured directions are radially positioned, centred by the steepest direction (dip direction) at 45 degree intervals. Since JRC values are highly dependent on the measurement scales, the measurements were performed in different window sizes ranging from 150 mm to 1000 mm in this study. The measurement window positions were determined in accordance with the locations of exposed joints, where the joints are distinctly exposed on the rock surfaces. The JRC values were estimated using roughness profiles which were extracted by the photogrammetric code, Sirovision. This program provides a function which estimates JRC values by selecting the corners of a specific area on the 3D model. The calculations are then carried out based on Eq.(1) and (2).

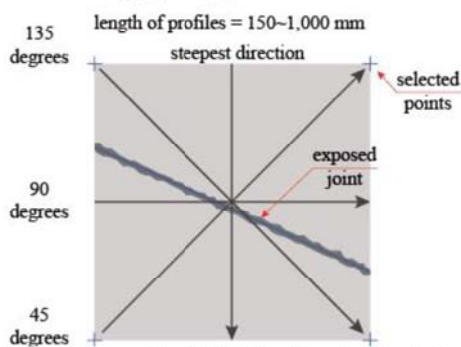


Figure 8 Selected areas for JRC estimation in Sirovision and the directions for directional JRCs

6. RESULTS AND DISCUSSION

6.1 JRC variation rates

The JRC values obtained from the 3D models at two yearly intervals using 'Sirovision' were analysed to estimate the JRC variation rates between the models. In two years, the variation rates have been changed from -0.45 (decreasing to 45% of previous JRC values) to 0.8 (increasing to 180% of previous JRC values). Figure 9 presents the JRV values in accordance with the measurement scales. Overall JRC data were formed with scattered patterns for both shale and sandstone zones. It is obvious that the strength of the relationships between JRV and measurement scale is "weak" or "moderate". The data distributions of the shale sections show weak correlations with the measurement scales ($R_2 = 0.02$). However, negative associations between the variables are also noticeable in the distributions. In the sandstone zone, the data distribution shows moderate positive correlations between JRV values and measurement scales ($R_2 = 0.12$).

It is interesting that an increase of JRC values by weathering is dominant in the shale zone rather than the sandstone sections. This is due to the different breaking patterns from the rock surfaces as mentioned in Section 5.3. In the small measurement scale range ($L = 150 \sim 300$ mm), on the other hand, a considerable amount of data from the sandstone zone shows a decrease of JRC values for two years. This can be explained by the fact that the loss of small scale roughness is more influential on the JRC values when the changes of undulations are negligible. To address the changes of JRC values, each example of the alteration of roughness profiles for both rock types is demonstrated in Figure 10.

The roughness profiles composed of regenerated 2 mm interval coordinates are shown in Figure 10. It is worth mentioning that the accuracy of photogrammetric JRC values is beyond the scope of this study. Generally, photogrammetric JRC values tend to be underestimated in the data interval (2 mm) compared to manually measured values. The accuracy of photogrammetric JRCs can vary with a quadratic function which depends on the camera-to-object distance and the employed focal lengths of lenses (Kim et al., 2015). However, this study compares the JRC values in the same density data condition.

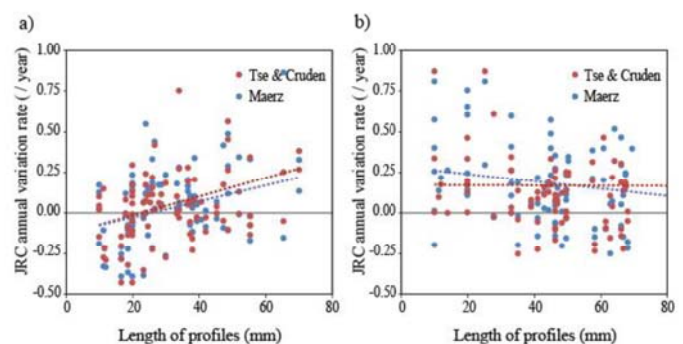
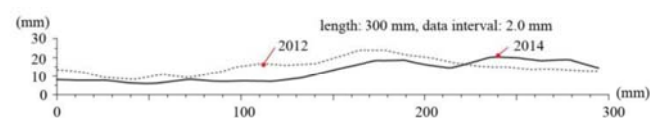


Figure 9 JRC variation rate according to the scales of profiles, shale (a), sandstone (b)

a) shale



b) sandstone

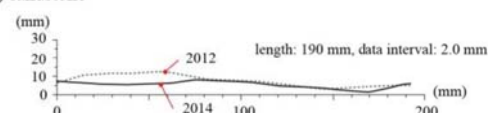


Figure 10 Examples of roughness profiles, shale (a) and sandstone (b)

6.2 Statistical indices for weathering

Based on the JRV data, the distributions of JRV according to the estimation functions (Tse&Cruden, 1979; Maerz, 1990) were plotted and the statistical indices were calculated. Figure 11 demonstrates that most data distributions form skewed distribution curves. It is obvious that the statistical results show the differences of JRV values between shale and sandstone. In the shale zone, the surface of the selected area has considerably changed due to the exfoliations controlled by the textural properties of the shale bedding structures as shown in Figure 6 (a) and (b). This has resulted in increasing of JRC values. The JRV distributions indicate higher average values ($\mu = 0.17 \sim 0.19$) (see Fig. 11 (a), (b)) than those of sandstone distributions ($\mu = 0.03 \sim 0.05$) (see Fig. 11 (c), (d)). The distribution of sandstone data is moved toward negative portions of the JRC variation rates. These negative data probably reflect the smoothly eroded rock surface profiles.

As the indicators of weathering for describing roughness variations, “mean” and “skew” values of JRC variation rates are used in this study. The mean values indicate the increased roughness of surfaces resulting in an increase of JRC values for one year. The geological structures of rocks have a strong influence on the values as well as the strengths of rocks. As shown in this study, the stepped roughness profiles of the shale zone produced larger JRV values than the sandstone sections, even though the shale samples have higher strength properties (UCS and Id_2) than those of the sandstone. As shown in section 5.3, the geological characteristic of shale, i.e. the exfoliations, which are composed of similarly shaped broken particles with thin and flat flakes, resulted in sharp edges on the surfaces. Therefore, the mean values of JRV can be used to describe a time dependent roughness variations in terms of the strength and geological characteristics of rocks.

However, a quantitative explanation of the skewness of JRV is complicated. The authors regard the skewness of the roughness distributions in this study as the tendency of data deviation from the mean values. In Figure 11, JRV data of all these analysis cases form positive skewed histograms, which means asymmetrical distributions with long tails can be expected from the considerably increased JRC values. A large value of skewness can indicate a large range of data sets which may be caused by geological differences between the data sets as well as the locality of the data sets. Further studies may be needed to identify the skewness of JRV data. It is interesting that JRV values increase with the slake durability index (Id_2) values of the rocks. This trend is different from the general understanding of the durability of rock material. In the study area, the durability of the shale sample is larger than the durability of sandstone data. However, the statistics indicate that the roughness alteration on the shale samples is larger than that of the sandstone samples. The relationships between the mean values of JRV and the Id_2 values of the shale and the sandstone zones are demonstrated in Figure 12. To compare the statistical indices of JRV data with the durability of both rock types, relevant properties are summarized in Table 2.

Table 2 Statistical indices of JRC variation rates for shale and sandstone and strength properties

Data distribution indices	JRC variation rates			
	Shale		Sandstone	
	Tse&Cruden	Maerz	Tse&Cruden	Maerz
no. of data	92	92	93	93
mean	0.17	0.19	0.03	0.05
standard deviation	0.33	0.28	0.20	0.24
median	0.132	0.143	0.021	0.043
mode	0.871	0.809	-0.43	-0.391
skew	2.604	1.103	0.466	1.042

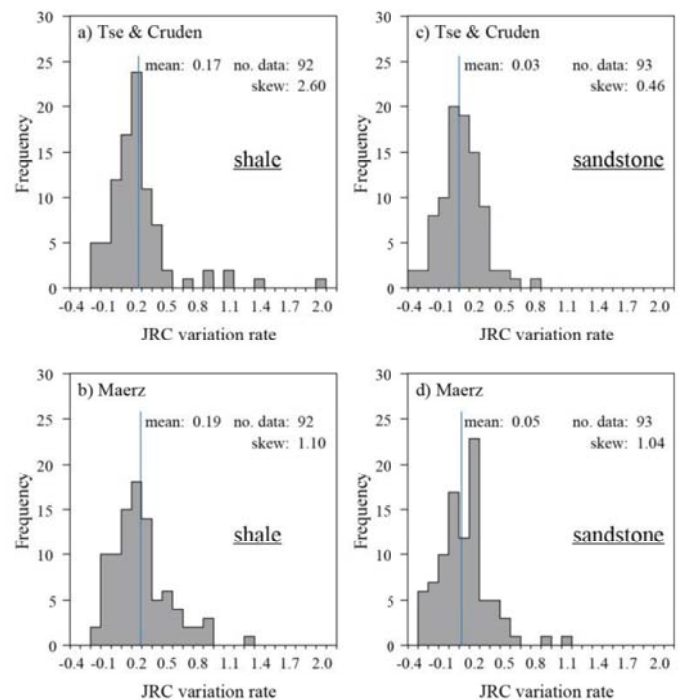


Figure 11 Histograms of JRC variation rates obtained using Tse&Cruden function (Eq. (1)), shale (a), sandstone (c); Maerz (Eq. (2)), shale (b), sandstone (d)

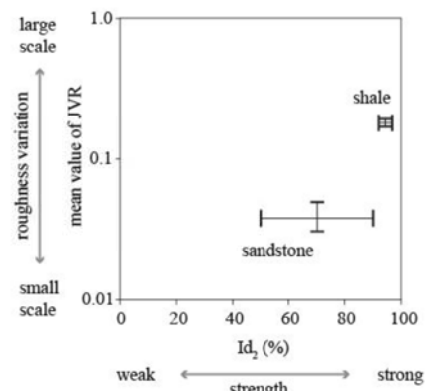


Figure 12 Correlations between mean values of JRC variation rates and Id_2 values for each rock type

6.3 Future works

The quantification for weathering is a challenging topic as the study of weathering is usually constrained by the slow rates of rock weathering. The suggested methodology in this study should be supported by further photogrammetry surveys for long periods to be verified. Weathering assessment in this study was performed relying on visual observations for the annual changes of rock surface recession. However, the weathering patterns vary with their geological characteristics derived from chemical and physical weathering environment. The weathering patterns in accordance with the rock types should be considered in future works.

7. CONCLUSION

The weathering characteristics of shale and sandstone in a cut slope within the Naranleigh-Fernvale beds in Australia, was investigated by an analysis based on historical photogrammetry surveys. In both the shale and sandstone zones of the study area, JRC data were collected over two years. With the comparisons of the JRC data, the present study suggests the use of the joint roughness variation rate (JVR) to show the annual changes of JRC values for a rock surface area. Through a statistical analysis, it was found that JVR values

indicate the alterations of rock surfaces caused by weathering in a short term.

As a result, the mean values of JVR were considerably different according to the rock types (shale: 0.17 ~ 0.19, sandstone: 0.03 ~ 0.05). This study shows that the “mean” of JVR values can be used as an indicator for quantifying the weathering degree of rocks while also considering the slake durability index (Id_2) in terms of both geological and mechanical characterizations.

8. ACKNOWLEDGEMENT

This research was performed with the financial support of the Griffith University International Postgraduate Research Scholarship program. The authors wish to thank Mr. George Poropat from CSIRO for the valuable assistance.

9. REFERENCES

- Arikan, F., Ulusay, R., Aydin, N. (2007) "Characterization of weathered acidic volcanic rocks and a weathering classification based on a rating system", *Bulletin of Engineering Geology and the Environment*, 66, pp415-430.
- Broch, E. and Franklin, J. A. (1972) "The point load strength test", *International Journal of Rock Mechanics and Mining Sciences*, 9, pp669-697.
- Cai, M., Kaiser, P. K. (2006) "Visualization of rock mass classification systems", *Geotechnical and Geological Engineering*, 24, pp1089-1102.
- CSIRO (2012) "Field procedures for photogrammetric pit mapping", CSIRO Exploration & Mining
- Ehlen, J. (1999) "Fracture characteristics in weathered granites", *Geomorphology*, 31, pp29-45.
- Gómez-Pujol, L., Fornós, J. J., and Swantesson, O. H. (2006) "Rock surface millimeter-scale roughness and weathering of supratidal Mallorcan carbonate coasts (Balearic Islands)", *Earth Surface Processes and Landforms*, 31, pp1792-1801.
- Gratchev, I., Shokouhi, A., Kim, D., Stead, D., Wolter, A. (2013) "Assessment of rock slope stability using remote sensing technique in the Gold Coast area, Australia", *Proceedings of the 18th Southeast Asian geotechnical and inaugural AGSSEA conference*, pp729-734.
- Hoek, E., Brown, E. T. (1997) "Practical estimates of rock mass strength", *International Journal of Rock Mechanics and Mining Sciences & Geomechanics Abstracts*, 27, pp329-343.
- ISRM (1978) "Suggested methods for the quantitative description of discontinuities in rock masses", *International Journal of Rock Mechanics and Mining Sciences*, 8, pp1165-1186.
- Kim, D. H., Gratchev, I., Balasubramaniam, A. S. (2013) "Determination of joint roughness coefficient (JRC) for slope stability analysis: a case study from the Gold Coast area, Australia", *Landslides*, 10, pp657-664.
- Kim, D. H., Gratchev, I., Balasubramaniam, A. S. (2014) "A photogrammetric approach for stability analysis of weathered rock slopes", *Geotechnical and Geological Engineering*, 33, pp443-454.
- Kim, D. H., Poropat, G. V., Gratchev, I., Balasubramaniam, A. S. (2015) "Improvement of photogrammetric JRC data distributions based on parabolic error models", *International Journal of Rock Mechanics and Mining Sciences*, <http://dx.doi.org/10.1016/j.ijrmms.2015.09.007>
- Maerz, N. H., Franklin, J. A., Bennett, C. P. (1990) "Joint roughness measurement using shadow profilometry", *International Journal of Rock Mechanics and Mining Sciences & Geomechanics Abstracts*, 27, pp329-343.
- Marinos, V., Marinos, P., Hoek, E. (2005) "The geological strength index: applications and limitations", *Bulletin of Engineering Geology and the Environment*, 64, pp55-65.
- McCarroll, D., and Nesje, A. (1996) "Rock surface roughness as an indicator of degree of rock surface weathering", *Earth Surface Processes and Landforms*, 21, pp963-977.
- Medapati, R. S., Kreidl, O. P., MacLaughlin, M., Hudyma, N., and Harris, A. (2013) "Quantifying surface roughness of weathered rock – examples from granite and limestone", *Proceedings of Geo-Congress 2013: Stability and performance of slopes and embankments III*, San Diego, California, pp120-128.
- Palmström, A. (2001) "In-situ characterization of rocks", A. A. Balkema Publishers, Lisse/Abingdon/Exton(PA)/Tokio.
- Pinho, A., Rodrigues-Carvalho, J., Gomes, C., and Duarte, I. (2006) "Overview of the evaluation of the state of rock weathering by visual inspection", *IAEG 2006 Engineering Geology for Tomorrow's Cities*, The Geological Society of London, paper 260
- Poropat, G. V. (2006) "Remote 3D mapping of rock mass structure", *Proceedings of the workshop of Laser and photogrammetric methods for rock face characterization*, Colorado, pp63-75.
- Poropat, G. V. (2009) "Measurement of surface roughness of rock discontinuities", *Proceedings of the 3rd CANUS rock mechanics symposium*, Toronto, Canada, paper 3976.
- Tse, R., Cruden, D. M. (1979) "Estimating joint roughness coefficients", *International Journal of Rock Mechanics and Mining Sciences & Geomechanics Abstracts*, 16, pp303-307.
- White, K., Bryant, R., and Drake, N. (1998) "Techniques for measuring rock weathering: application to a dated fan segment sequence in southern Tunisia", *Earth Surface Processes and Landforms*, 23, pp1031-1043.